Available online at www.sciencedirect.com
SCIENCE DIRECT
International Journal of Heat and Mass Transfer 49 (2006) 3855–3865
International Journal of HEAT and MASS TRANSFER
www.elsevier.com/locate/ijhmt

Mechanical and thermal characteristics of a mixed convection boundary-layer flow in a saturated porous medium

E. Magyari [a], Emad H. Aly [b,*]

[a] Chair of the Physics of Buildings, Institute of Building Technology, Swiss Federal Institute of Technology (ETH) Zürich, Wolfgang-Pauli-Street 1, CH-8093 Zürich, Switzerland
[b] Department of Civil and Building Engineering, Loughborough University, Loughborough LE11 3TU, UK

Received 22 June 2005
Available online 30 June 2006

Abstract

The mixed convection over a vertical surface adjacent to a fluid saturated porous medium and having the temperature distribution $T_w(x) = T_\infty + T_0 \cdot (x/L)^\lambda$ is considered in the boundary-layer and Boussinesq approximation for the value $\lambda = -1/3$ of the power-law exponent. It is shown that in the whole range $-\infty < \varepsilon < +\infty$ of the mixed convection parameter ε an infinite number of solutions exist which are associated with different values of the dimensionless wall temperature gradient $\theta'(0) \equiv h$. These solutions are investigated analytically and numerically in detail. The effect of a thermodynamic requirement on the existence domain of the physical solutions is discussed in the context of results reported by other authors.

Keywords: Mixed convection; Boundary-layer; Porous medium; Heat transfer; Multiple solutions; Existence domain

1. Introduction

The problem of the mixed convection over a vertical flat plate plays the role of a basic paradigm both for the viscous flow of clear fluids as well as for the flow in fluid saturated porous media. While the former topic has become a textbook matter more than 50 years ago, the latter one still belongs since the pioneering work of Cheng [1] to an active research field of our days. Important stations of this early development in exploring the mathematical features of the corresponding boundary value problem mark the contributions of Merkin [2,3]. Excellent reviews of the further development in the mixed convection in special and of that of the flows in saturated porous media in general, have been published recently by Nield and Bejan [4], Vafai [5], Pop and Ingham [6], Bejan and Kraus [7], Ingham et al. [8], Bejan et al. [9] and Vafai [10]. Further results concerning the mixed convection boundary-layer flows over a vertical plate in a porous medium have been reported recently by Aly [11], Aly et al. [12], Nazar et al. [13], Guedda [14] and Brighi and Hoernel [15].

In their comprehensive paper Aly et al. [12] have reviewed the previous work and extended the investigation of the basic features of the self-similar mixed convection boundary-layer flows past a thin vertical fin in a saturated porous medium which is maintained at a constant ambient temperature T_∞. The temperature distribution T_w of the fin has been assumed to be of the form

$$T_w(x) = T_\infty + T_0 \cdot \left(\frac{x}{L}\right)^\lambda, \tag{1}$$

where λ is a constant, x is the distance from the tip of the fin, L is a reference length and T_0 is the difference between the temperature of the fin at $x = L$ and the ambient temperature T_∞, $T_0 = T_w(L) - T_\infty$. The mainstream velocity at the outer edge of the boundary layer has also been assumed to vary as x^λ so that a similarity reduction of the basic equations could be performed. Assuming further that the boundary-layer and the Boussinesq approximations

* Corresponding author.
E-mail address: E.H.Aly@lboro.ac.uk (E.H. Aly).

0017-9310/$ - see front matter © 2006 Elsevier Ltd. All rights reserved.
doi:10.1016/j.ijheatmasstransfer.2006.05.003

Nomenclature

D	Dawson integeral
erf	the error function
f	similar stream function
g	magnitude of the acceleration due to gravity
h	similar surface temperature gradient
K	permeability of the porous media
k_m	thermal conductivity of the porous medium
L	reference length
M	Kummer's confluent hypergeometric function
Pe	Péclet number, $=U_0L/\alpha_m$
q_w	wall heat flux
Ra	Darcy-Rayleigh number, $=\rho g\beta KLT_0/(\mu\alpha_m)$
T	temperature

Greek symbols

α_m	effective thermal diffusivity of the porous medium
β	coefficient of thermal expansion
ε	mixed convection parameter, $=Ra/Pe$
η	dimensionless similarity variable, $=\sqrt{Pe/2}\cdot(x/L)^{\frac{\lambda-1}{2}}\cdot(y/L)$
μ	dynamic viscosity of the fluid
θ	similar temperature variable, $=(T-T_\infty)/(T_0(x/L)^\lambda)$
ρ	density
τ_w	wall shear stress

Subscripts

0	reference
m	parameters of porous media
w	condition at the wall
∞	condition at the free stream

hold, for the corresponding similar temperature field $\theta=\theta(\eta)$ and stream function $f=f(\eta)$ the following boundary value problem has been obtained

$$\theta''+(1+\lambda)f\cdot\theta'-2\lambda f'\theta=0,\qquad f'=1+\varepsilon\theta, \tag{2a, b}$$

$$f(0)=0,\quad \theta(0)=1,\quad \theta(\infty)=0. \tag{3a, b, c}$$

Here the primes denote derivatives with respect to the similarity variable η and ε stands for the ratio of the Darcy-Rayleigh number and the Péclet number, $\varepsilon=Ra/Pe$. Positive and negative values of ε correspond to the aiding (hot plate, $T_0>0$) and opposing (cold plate, $T_0<0$) mixed convection flows, respectively, while $\varepsilon=0$ corresponds to the forced convection case. Since (in the model) no heat sources and sinks are present, the temperature of the fluid in the aiding case may nowhere be lower than the ambient temperature T_∞, and in the opposing case it may nowhere be higher than T_∞. This physical requirement leads to the important additional condition for the similar temperature field

$$\theta(\eta)>0,\quad \text{for } 0\leqslant\eta<\infty. \tag{4}$$

The mechanical and thermal characteristics of the mixed convection flow, namely the (dimensional) velocity and temperature fields $\mathbf{v}=(u,v,0)$ and $T(x,y)$, the wall shear stress $\tau_w(x)$ as well as the wall heat flux $q_w(x)$ can all be expressed in terms of $f=f(\eta)$, $\theta=\theta(\eta)$ and of their derivatives as these are listed in Appendix A.

The aim of the present paper is to investigate the mixed convection problem for the value $\lambda=-1/3$ of the power-law exponent in detail and to emphasize the effect of the physical requirement (4) on the solutions of the boundary value problem (2) and (3). The option for this special value of λ is motivated by the existence for $\lambda=-1/3$ of a first integral of Eqs. (2) which lowers the order of the problem on one hand, and allows to obtain several analytical solutions on the other hand.

2. A first integral for $\lambda=-1/3$

Eq. (2a) can be transcribed in the form

$$\frac{d}{d\eta}(\theta'-2\lambda f\theta)=-(1+3\lambda)f\theta'. \tag{5}$$

This equation shows that our problem admits for $\lambda=-1/3$ the first integral $\theta'-2\lambda f\theta=\text{const}$. The boundary conditions (3a) and (3b) imply that the integration constant is nothing more than the similar wall temperature gradient

$$\theta'(0)\equiv h. \tag{6}$$

Thus, for $\lambda=-1/3$ the problem (2) and (3) reduces to the lower order initial value problem

$$\theta'+\frac{2}{3}f\theta=h,\qquad f'=1+\varepsilon\theta,\qquad \theta(0)=1,\quad f(0)=0, \tag{7a, b, c, d}$$

along with the additional conditions (3c) and (4),

$$\theta(\infty)=0\quad\text{and}\quad\theta(\eta)>0\qquad\text{for } 0\leqslant\eta<\infty. \tag{8a, b}$$

Taking into account that $\theta'(\infty)=0$ (no heat may escape to infinity) from Eq. (7a) we obtain

$$h=\frac{2}{3}\lim_{\eta\to\infty}(f\theta). \tag{9}$$

In spite of the boundary condition (3c), the value of h as given by (9) is not necessarily zero. It is only so if $\theta(\eta)$ goes

to zero faster than $f(\eta)$ goes to infinity as $\eta \to \infty$. In this case no heat is transferred between the surface and the fluid (except for the leading edge singularity). When, however $\theta(\eta)$ and $1/f(\eta)$ decay with the same rate as $\eta \to \infty$, the limit (9) may become finite and a heat transfer process takes place in every point of the surface. Therefore, in the investigation of the problem (2)–(4) for $\lambda = -1/3$, two physically relevant cases $h = 0$ and $h \neq 0$ have to be distinguished, respectively. This will be done in Sections 4 and 5 in detail.

Having in mind that Eqs. (7) specify an initial value problem, we conclude that

(i) it admits solution for any given values of h and ε,
(ii) this solution is unique, and
(iii) this solution of Eqs. (7) solves our physical problem only if it also satisfies the additional conditions (8a,b).

3. Forced convection solutions

In the forced convection case $\varepsilon = 0$ the boundary value problem (2) and (3) admits for the similar stream function for the any value of λ the uniform solution

$$f(\eta) = \eta, \tag{10}$$

Thus, for the similar temperature field the following linear boundary value problem results,

$$\theta'' + (1+\lambda)\eta\theta' - 2\lambda\theta = 0, \quad \theta(0) = 1, \quad \theta(\infty) = 0. \tag{11a,b,c}$$

For an uniform main stream, $\lambda = 0$, one immediately recovers the well known error function solution

$$\theta(\eta) = 1 - \mathrm{erf}\left(\frac{\eta}{\sqrt{2}}\right), \quad \theta'(0) = -\sqrt{\frac{2}{\pi}} \quad (\lambda = 0). \tag{12a,b}$$

For the similarity exponent $\lambda = -1/3$ considered in the present paper, Eq. (11a) reduces to Eq. (7a). Thus one easily obtains that the problem (7) admits the family of multiple solutions

$$\theta(\eta) = \mathrm{e}^{-\frac{\eta^2}{3}} + \sqrt{3}\cdot h \cdot D\left(\frac{\eta}{\sqrt{3}}\right) \quad (\lambda = -1/3), \tag{13a}$$

where D denotes the Dawson integral (see Abramowitz and Stegun [16], Chapter 7),

$$D(z) = \mathrm{e}^{-z^2}\int_0^z \mathrm{e}^{+t^2}\,\mathrm{d}t. \tag{14}$$

We mention that θ given by Eq. (13a) can also be expressed in terms of Kummer's confluent hypergeometric functions $M(a,b,z)$ (see Abramowitz and Stegun [16], Chapter 13) as follows:

$$\theta(\eta) = \mathrm{e}^{-\frac{1}{3}\eta^2}\left[1 + h\cdot\eta\cdot M\left(\frac{1}{2},\frac{3}{2},\frac{1}{3}\eta^2\right)\right]. \tag{13b}$$

In Eqs. (13) the constant of h is arbitrary, but the physical requirement (4) restricts it to non-negative values, $h \geqslant 0$. In the special case $h = 0$ one obtains the elementary closed form solution

$$\theta(\eta) = \mathrm{e}^{-\frac{\eta^2}{3}} \quad (\lambda = -1/3,\ \ h = 0). \tag{15}$$

Hence, for $h = 0$ the similar temperature $\theta(\eta)$ possesses a very fast exponential decay. For $h \neq 0$, however, its asymptotic behavior is dominated by the second term on the right-hand side of Eqs. (13). Since $D(z) \to 1/(2z)$ as $z \to \infty$, we obtain that $\theta(\eta)$ decays algebraically according to

$$\theta(\eta) \to \frac{3h}{2\eta} \quad \text{as } \eta \to \infty. \tag{16}$$

Therefore, in the case ($\lambda = -1/3$, $\varepsilon = 0$) our physical problem admits an infinite number of solutions, one solution (13) for any non-negative value of h. This finding is in full agreement with the general result reported by of Guedda [14], valid for $\{-1 < \lambda < 0,\ -1 < \varepsilon < 1/2\}$. Our one-parameter family of solutions (13) decays algebraically according to Eq. (16) for $h > 0$ and exponentially according to Eq. (15) for $h = 0$. This example emphasizes the remarkable feature, how a one-parameter family of algebraically decaying boundary-layers may go over in an exponentially decaying boundary-layer gradually (in the present case, as $h \to 0$).

4. Solutions for $h = 0$

In the following considerations of the present paper we assume throughout that $\varepsilon \neq 0$. The solutions of the initial value problem (7) along with the additional conditions (8) will be investigated numerically and analytically for $h = 0$ (present Section) and $h \neq 0$ (Section 5), respectively.

4.1. Numerical solutions for $h = 0$

The initial value problem (7) can easily be solved numerically with the aid of any standard library program. In Fig. 1 the shapes of the similar stream function $f = f(\eta)$ obtained by such a numerical integration of the problem (7) for $h = 0$ and different values of the parameter ε are shown. Figs. 2 and 3 show the corresponding similar velocity and temperature profiles $f' = f'(\eta)$ and $\theta = \theta(\eta)$, respectively. All these profiles satisfy also the additional conditions (8a,b).

The numerical calculations indicate that for $h = 0$ the solution of the initial value problem (7)

(i) satisfies the two additional conditions (8) for any given value of ε in the range $\varepsilon > -1$, but
(ii) in the range $\varepsilon \leqslant -1$ it does not satisfy either of the two conditions (8).

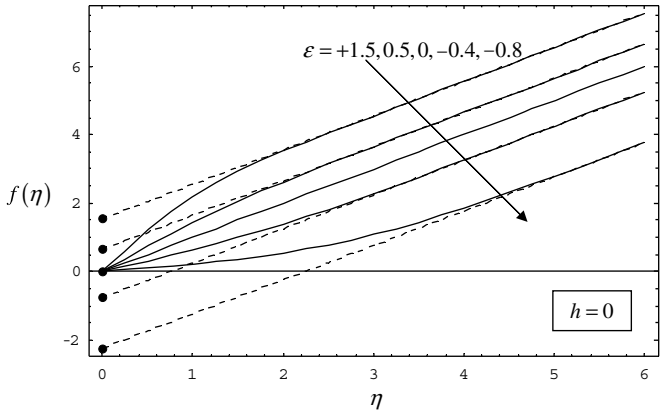

Fig. 1. Profiles of the similar stream function $f = f(\eta)$ for different values of the mixed convection parameter ε. The dashed lines show the asymptotes and the dots mark the intersection points $f_\infty(\varepsilon)$ of the asymptotes with the vertical axis. From top to bottom: $f_\infty(\varepsilon) = 1.54757$, 0.64645, 0, −0.75391, −2.23878.

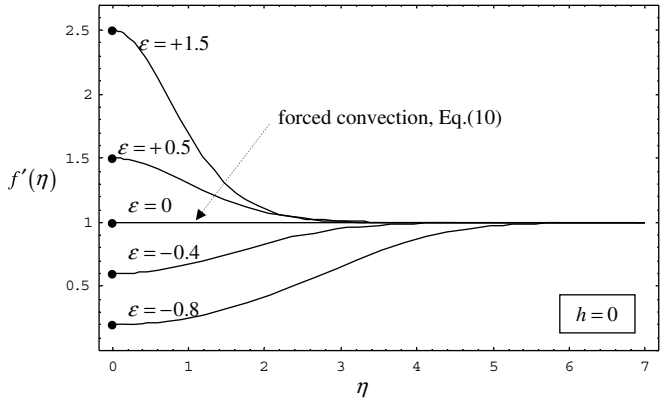

Fig. 2. Shape of the velocity profiles $f' = f'(\eta)$ for different values of the parameter ε. The dots mark the initial values $f'(0) = 1 + \varepsilon$.

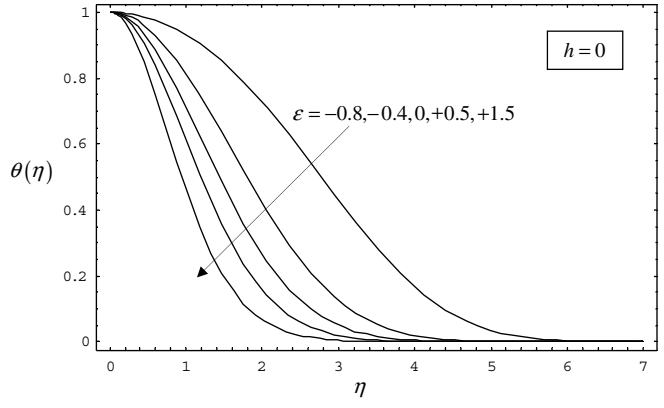

Fig. 3. Shape of the similar temperature profiles $\theta = \theta(\eta)$ for different values of the parameter ε.

Hence, for $h = 0$ our problem (7) and (8) admits solutions only for $\varepsilon > -1$ and these solutions are unique.

4.2. Approximate analytical solutions for $h = 0$

Integrating Eq. (7a) once and taking into account Eq. (7c) one immediately obtains

$$\theta(\eta) = \exp\left(-\frac{2}{3}F(\eta)\right), \tag{17}$$

where

$$F(\eta) \equiv \int_0^\eta f(\tilde{\eta})\,\mathrm{d}\tilde{\eta}. \tag{18}$$

Thus, according to Eq. (7b) we obtain for the similar downstream velocity the expression

$$f'(\eta) = 1 + \varepsilon \exp\left(-\frac{2}{3}F(\eta)\right). \tag{19}$$

Eq. (19) can now be solved by successive approximations according to the scheme

$$f'_{n+1}(\eta) = 1 + \varepsilon \exp\left(-\frac{2}{3}F_n(\eta)\right), \quad n = 0, 1, 2, \ldots, \tag{20}$$

where

$$F_n(\eta) = \int_0^\eta f_n(\tilde{\eta})\,\mathrm{d}\tilde{\eta}. \tag{21}$$

Starting the iteration with the zeroth-order trial function $f_0(\eta) = 0$, we obtain in the first-order approximation

$$f'_1(\eta) = 1 + \varepsilon. \tag{22}$$

Having in mind Eqs. (7d) and (18) we further obtain

$$f_1(\eta) = (1 + \varepsilon)\eta, \tag{23a}$$

$$F_1(\eta) = \frac{1}{2}(1 + \varepsilon)\eta^2, \tag{23b}$$

In the second-order approximation we have

$$f'_2(\eta) = 1 + \varepsilon \exp\left(-\frac{2}{3}F_1(\eta)\right) = 1 + \varepsilon \exp\left(-\frac{1}{3}(1 + \varepsilon)\eta^2\right) \tag{24}$$

and thus

$$f_2(\eta) = \eta + \frac{\varepsilon}{2}\sqrt{\frac{3\pi}{1+\varepsilon}} \cdot \mathrm{erf}\left(\sqrt{\frac{1+\varepsilon}{3}} \cdot \eta\right), \tag{25}$$

which further implies

$$F_2(\eta) = \frac{\eta^2}{2} + \frac{3\varepsilon\sqrt{\pi}}{2(1+\varepsilon)}\left[\sqrt{\frac{1+\varepsilon}{3}} \cdot \eta \cdot \mathrm{erf}\left(\sqrt{\frac{1+\varepsilon}{3}} \cdot \eta\right) - \frac{1 - \exp\left(-\frac{1+\varepsilon}{3}\eta^2\right)}{\sqrt{\pi}}\right]. \tag{26}$$

Accordingly, in the third-order approximation we obtain for $f'(\eta)$ the expression

$$f'_3(\eta) = 1 + \varepsilon \exp\left(-\frac{2}{3}F_2(\eta)\right), \tag{27}$$

with $F_2(\eta)$ given by Eq. (26). The corresponding similar temperature field is

$$\theta(\eta) = \exp\left(-\frac{2}{3}F_2(\eta)\right). \tag{28}$$

This third-order approximation for θ reproduces the temperature profiles shown in Fig. 3 with a high accuracy. The expressions Eqs. (23b) and (26) of $F_n(\eta)$ also show that the solutions exist only for $\varepsilon > -1$, but for $\varepsilon \leqslant -1$ the condition (3c) is violated. Moreover, in the special case of the forced convection, $\varepsilon = 0$, one immediately recovers in (28) the exact elementary solution (15). Furthermore, Eq. (25) shows that for the coordinates $f_\infty(\varepsilon)$ of the intersection points of the asymptotes plotted by dashed lines in Fig. 1 can be calculated from the approximation formula:

$$f_\infty(\varepsilon) = \frac{\varepsilon}{2}\sqrt{\frac{3\pi}{1+\varepsilon}}. \tag{29}$$

The smaller $|\varepsilon|$ is taken the higher accuracy of (29) is obtained. For $\varepsilon = +0.5$ and $\varepsilon = -0.4$, e.g., it yields $f_\infty(\varepsilon) = +0.626657$ and $f_\infty(\varepsilon) = -0.792665$ which are quite close to the exact values specified in the caption of Fig. 1.

4.3. Implicit analytical solution for the similar stream function

For $\varepsilon \neq 0$ the similar temperature θ can be eliminated with the aid of Eq. (2b) from all the governing equations. Thus, the (trivially) coupled initial value problem (7) reduces to the (second order) initial value problem

$$\begin{aligned} &f'' + \frac{2}{3}f(f'-1) = \varepsilon h, \\ &f(0) = 0, \quad f'(0) = 1+\varepsilon, \end{aligned} \tag{30a, b, c}$$

for the similar stream function f. The additional conditions (8a,b) read in this case

$$f'(\infty) = 1 \quad \text{and} \quad \operatorname{sgn}[f'(\eta)-1] = \operatorname{sgn}\varepsilon \quad \text{for } 0 \leqslant \eta < \infty. \tag{31a, b}$$

Eq. (30) can be transcribed into the form

$$f'\frac{\mathrm{d}f'}{\mathrm{d}f} + \frac{2}{3}f(f'-1) = \varepsilon h, \tag{32}$$

where f plays the role of a new independent and f' that of a new dependent variable.

For $h = 0$, Eq. (32) can easily be integrated once by separation of variables f and f'. In this way, the second-order problem (30) reduces to the first-order one

$$\begin{aligned} &f' = 1 + \varepsilon\exp\left(1+\varepsilon-\tfrac{1}{3}f^2\right)\exp(-f'), \\ &f(0) = 0, \end{aligned} \tag{33a, b}$$

along with the same additional conditions (31).

Now, we first solve Eq. (33a) for f' with the aid of the Lagrange-expansion method (see Appendix B) to obtain

$$\begin{aligned} &f' = 1 + G(f), \\ &G(f) = \sum_{n=1}^{\infty}\frac{(-1)^n n^{n-1}}{n!}\varepsilon^n \exp\left[n\left(\varepsilon - \frac{1}{3}f^2\right)\right]. \end{aligned} \tag{34a, b}$$

In this way the similar stream function $f(\eta)$ can be obtained in the implicit form $\eta = \eta(f)$ by quadratures,

$$\eta = \int_0^f \frac{\mathrm{d}z}{1-G(z)}. \tag{35}$$

By increasing the number of the terms taken into account in $G(f)$, Eq. (35) reproduces the curves of Fig. 1 with increasing accuracy. Breaking down the sum in $G(f)$ after its first term, Eq. (35) becomes

$$\eta = \int_0^f \frac{\mathrm{d}z}{1+\varepsilon\exp\left(\varepsilon - \frac{1}{3}z^2\right)} \tag{36}$$

and furnishes a good approximation for $|\varepsilon| \ll 1$. In this range of ε, the integral in (36) can be approximated as follows:

$$\eta = f - \frac{\sqrt{3\pi}}{2}\varepsilon\cdot\exp(\varepsilon)\cdot\operatorname{erf}\left(\frac{f}{\sqrt{3}}\right) \quad (|\varepsilon| \ll 1). \tag{37}$$

This approximation can further be improved by expanding the integrand in Eq. (35) in a power series of G,

$$\eta = f + \int_0^f \left[G(z) + G^2(z) + G^3(z) + \cdots\right]\mathrm{d}z \quad (|\varepsilon| \ll 1). \tag{38}$$

Similarly to Eq. (37), all integrals present in Eq. (38) can be expressed in terms of error functions. Collecting the terms of the same powers of $\varepsilon\exp(\varepsilon)$, the result to the order $\varepsilon^4\exp(4\varepsilon)$ reads

$$\begin{aligned} \eta = f &- \frac{\sqrt{3\pi}}{2}\varepsilon\exp(\varepsilon)\operatorname{erf}\left(\sqrt{\frac{1}{3}}\cdot f\right) \\ &+ \frac{\sqrt{6\pi}}{2}\varepsilon^2\exp(2\varepsilon)\operatorname{erf}\left(\sqrt{\frac{2}{3}}\cdot f\right) \\ &- \frac{9\sqrt{\pi}}{4}\varepsilon^3\exp(3\varepsilon)\operatorname{erf}\left(\sqrt{\frac{3}{3}}\cdot f\right) \\ &+ 8\sqrt{\frac{\pi}{3}}\varepsilon^4\exp(4\varepsilon)\operatorname{erf}\left(\sqrt{\frac{4}{3}}\cdot f\right) \quad (|\varepsilon| \ll 1). \end{aligned} \tag{39}$$

5. Solutions for $h \neq 0$

5.1. Numerical solutions for $h \neq 0$

When $h \neq 0$, the features (i)–(iii) listed at the end of Section 2 are still valid, but the parameter space of our initial value problem (7) becomes two-dimensional; it is now the plane (ε, h). The numerical solution procedure is basically the same as in the case $h = 0$.

The results for the existence of physical solutions satisfying the additional conditions (8) (and associated with $h = 0$

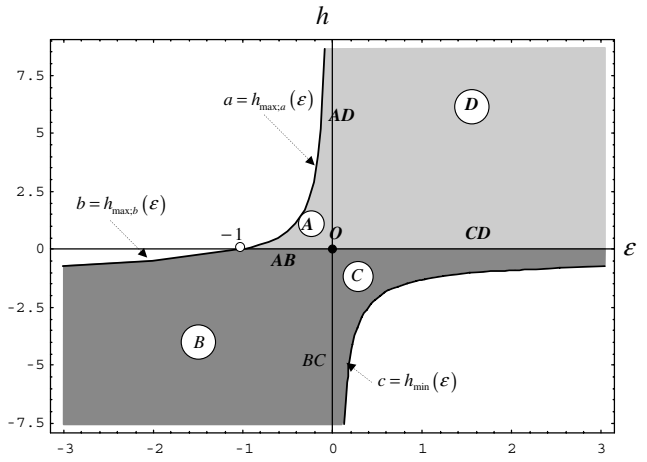

Fig. 4. Existence domain (40) and (41) of the physical and non-physical solutions of the boundary values (7) and (8), respectively, in the parameter plane (ε,h). These domains are highlighted by grey (physical) and by dark grey (non-physical), respectively. The point $(-1,0)$ does not belong to the solution domain of the boundary values (7) and (8).

and $h \neq 0$, respectively) are represented in Fig. 4. For the sake of completeness, in Fig. 4 the existence domain of the non-physical solutions which do not satisfy the positiveness condition (8b) is also shown. The results can be summarized as follows.

1. Physical solutions exist only for the points which belong to the domain

$$CD \cup D \cup AD \cup A \cup AB \cup O, \tag{40a}$$

of the parameter plane (ε, h). For this domain the following inequalities hold:

$$h \geqslant 0 \quad \text{for } \varepsilon \geqslant 0, \tag{40b}$$

$$0 \leqslant h \leqslant h_{\max;a}(\varepsilon) \quad \text{for } -1 < \varepsilon < 0. \tag{40c}$$

2. From every point of the subdomains AB, O and CD (i.e. of the range $\varepsilon > -1$ of ε-axis) there bifurcates a family of physical solutions associated with all positive values of h between zero and $+\infty$ for $\varepsilon \geqslant 0$, and between zero and the branch $a = h_{\max;a}(\varepsilon)$ of the border curve, for $-1 < \varepsilon < 0$ respectively.
3. The existence domain of the non-physical solutions, i.e. of those solutions of the problem (7) and (8) which violate the positiveness condition (8b), is the set of points

$$B \cup BC \cup C, \tag{41a}$$

where the following inequalities hold

$$h_{\min;c}(\varepsilon) \leqslant h < 0 \quad \text{for } \varepsilon > 0, \tag{41b}$$

$$h < 0 \quad \text{for } -1 < \varepsilon \leqslant 0, \tag{41c}$$

$$h \leqslant h_{\max;b}(\varepsilon) < 0 \quad \text{for } \varepsilon < -1. \tag{41d}$$

4. In the forced convection case, $\varepsilon = 0$, both the family of physical and non-physical solutions corresponding to values $h \geqslant 0$ and $h < 0$ of the dimensionless wall temperature gradient, respectively, are available in an explicit analytical form, being given by Eqs. (13).
5. The point $(-1,0)$ does not belong to the solution domain.

The above results are illustrated in Figs. 4–7.

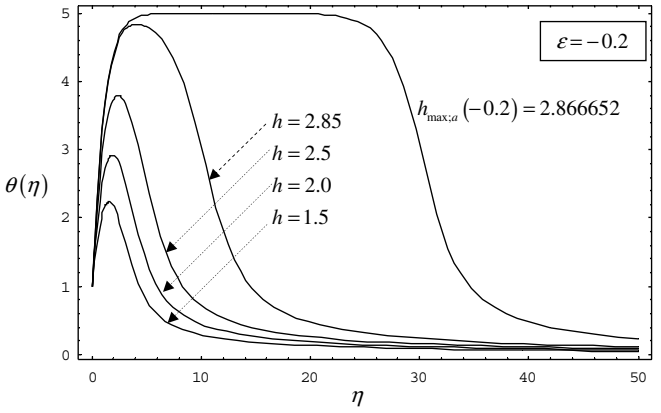

Fig. 5. Temperature profiles $\theta = \theta(\eta)$ in the subdomain A for $\varepsilon = -0.2$ and different values of h between 0 and $h = h_{\max;a}(-0.2) = 2.866652$.

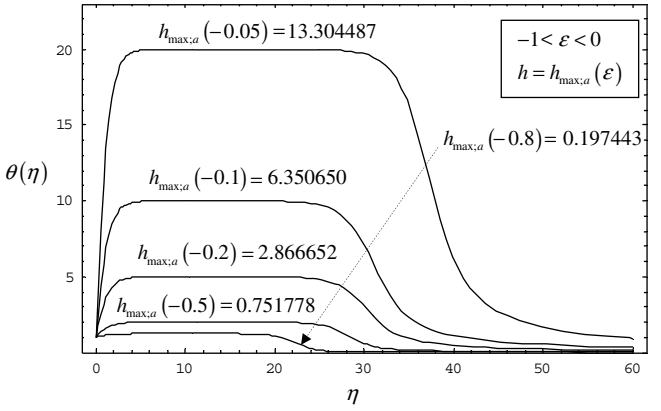

Fig. 6. Temperature profiles $\theta = \theta(\eta)$ corresponding to the points of the border curve $h_{\max;a}(\varepsilon)$ of the subdomain A shown in Fig. 4, for $\varepsilon = -0.05$, -0.1, -0.2, -0.5 and -0.8, respectively.

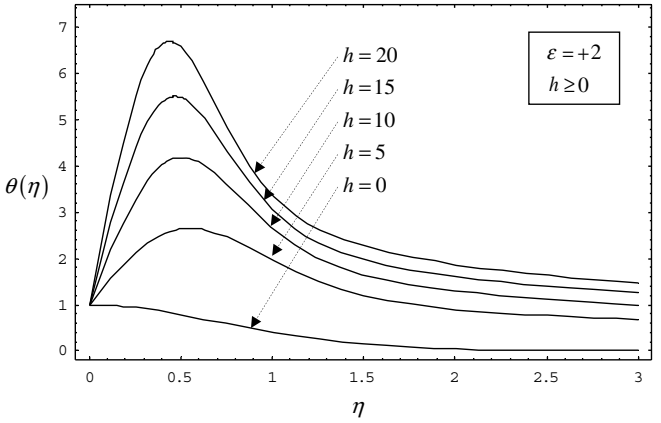

Fig. 7. Temperature profiles $\theta = \theta(\eta)$ for $\varepsilon = +2$ and different values of h between 0 and $+\infty$. In the range $\varepsilon \geqslant 0$ no upper bound exists for h.

5.2. Analytical solutions for $h \neq 0$

Our basic equation (7a) is a first-order linear non-homogeneous differential equation for θ. Its formal solution (we call it "formal", since $f=f(\eta)$ is still unknown) can easily be obtained by the standard method of the "variation of the constants". This solution, obeying the wall condition (7c) reads

$$\theta(\eta) = \exp\left[-\frac{2}{3}F(\eta)\right] \cdot \left(1 + h \cdot \int_0^\eta \exp\left[+\frac{2}{3}F(\bar{\eta})\right] \mathrm{d}\bar{\eta}\right), \tag{41}$$

where F is given by Eq. (18).

Now, the task is to determine the similar stream function $f=f(\eta)$ (involved in F) which solves the problem (30) with $h \neq 0$ and satisfies the additional conditions (31).

A straightforward way to do this is to search the solution in the form of a power series of η,

$$f(\eta) = \sum_{k=0}^{\infty} A_k \eta^k. \tag{42}$$

The boundary conditions (30b,c) as well as the obvious relationship

$$f''(0) = \varepsilon h, \tag{43}$$

imply immediately that

$$A_0 = 0, \quad A_1 = 1 + \varepsilon, \quad A_2 = \frac{\varepsilon h}{2}, \tag{44a, b, c}$$

Substituting Eq. (42) into Eq. (30a), we obtain the following recursion equations for the coefficients A_n,

$$A_n = \frac{2}{3n(n-1)}\left[A_{n-2} - \sum_{k=1}^{n-2}(n-k-1)A_k A_{n-k-1}\right], \quad n = 3, 4, 5, \ldots \tag{45}$$

The recursion equation (45) allow both for a rapid symbolical and numerical evaluation of the coefficients of the series (42) in terms of the first three of them which are given by Eqs. (44). Thus, for n running from 3 to 7, one obtains the expressions

$$A_3 = -\frac{\varepsilon(1+\varepsilon)}{9},$$

$$A_4 = -\frac{\varepsilon h(2+3\varepsilon)}{36},$$

$$A_5 = -\frac{9\varepsilon^2 h^2 - 2\varepsilon(1+\varepsilon)(3+4\varepsilon)}{540},$$

$$A_6 = \frac{\varepsilon h(25\varepsilon^2 + 32\varepsilon + 8)}{1620},$$

$$A_7 = \frac{27\varepsilon^2 h^2(5+7\varepsilon) - 2\varepsilon(1+\varepsilon)(34\varepsilon^2 + 48\varepsilon + 15)}{34020}. \tag{46a, b, c, d, e}$$

In this way,

$$F(\eta) = \sum_{k=1}^{\infty} \frac{A_k}{k+1}\eta^{k+1}. \tag{47}$$

In the convergence range of the series involved, Eq. (41) with F given by Eq. (47) yields the exact analytical solution of the problem (7). In the "grey region" of the parameter plane (ε, h) shown in Fig. 4, this solution satisfies also the additional conditions (8).

The rate of convergence of series (47) can often be accelerated with the aid of Euler's well known series transformation. On using an alternative form of this transformation which is due to Knopp [17], Eq. (47) may be rewritten as follows

$$F(\eta) = \sum_{k=1}^{\infty}\left[\frac{k!}{2^{k+1}} \cdot \sum_{m=1}^{\infty} \frac{A_m \cdot \eta^{m+1}}{(k-m)!(m+1)!}\right] \tag{48}$$

Obviously, for numerical evaluations the series present in the above equations must be truncated, such that Eq. (41) actually yields with (47) or (48) an approximate solution. One may expect that a suitable truncation of the series leads (at least for small values of η) to an accurate approximation. How this procedure works, will be illustrated below by a couple of examples.

5.2.1. First example

We first consider the special case of the forced convection which corresponds to $\varepsilon = 0$. In this case all the coefficients A_n are zero except for $A_1 = 1$. Thus, Eqs. (41) and (47) yield

$$\theta(\eta) = \exp\left(-\frac{1}{3}\eta^2\right)\left[1 + h \cdot \int_0^\eta \exp\left(+\frac{1}{3}\bar{\eta}^2\right)\mathrm{d}\bar{\eta}\right]. \tag{49}$$

It is easy to see that Eq. (49) coincides with the exact solution (13a) given in terms of Dawson's integral.

5.2.2. Second example

As a second illustration of the above method, in Figs. 8a and 8b the temperature profiles corresponding to the

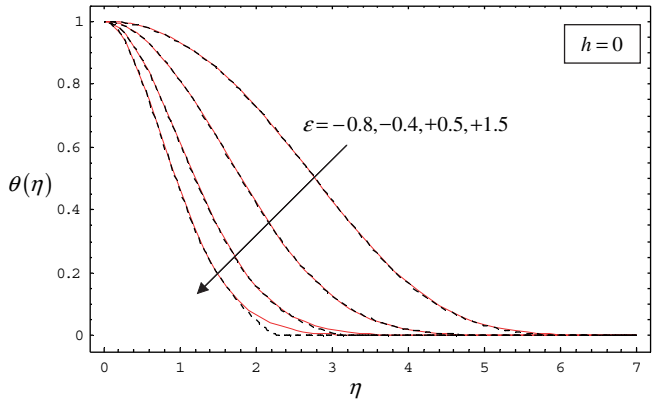

Fig. 8a. The similar temperature profiles $\theta = \theta(\eta)$ of Fig. 3 (full lines) as compared to those obtained from Eqs. (41) and (47) by truncating the series to polynomials of degree 13.

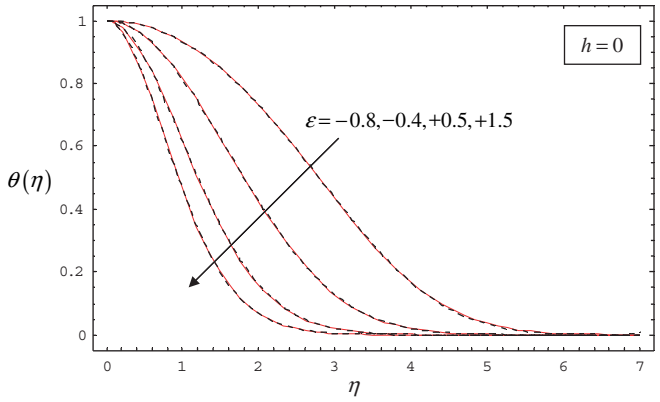

Fig. 8b. The similar temperature profiles $\theta = \theta(\eta)$ of Fig. 3 (full lines) as compared to those obtained from Eqs. (41) and (48) by truncating the series to polynomials of degree 12.

non-vanishing ε-values of Fig. 3 are compared with the same profiles obtained from Eq. (41) by using for F the expression (47) and (48), respectively. The series involved have been truncated to polynomials of degrees 13 and 12, respectively. As expected, the transformed expression (48) performs better than (47), especially in the neighborhood of the outer edge of the temperature boundary layers where in the former case the approximation is less accurate for $\varepsilon = 0.5$ and 1.5.

5.2.3. Third example

In Fig. 9 the "exact numerical" velocity profiles are compared to those obtained from Eqs. (41) and (48) by truncating the series to polynomials of degree 13 for $h = 0.1$ and four different values of ε. We see that the approximation procedure is still working also for a non-vanishing value of h, but its accuracy starts to become poor again in the neighborhood of the outer edge of the temperature boundary layers.

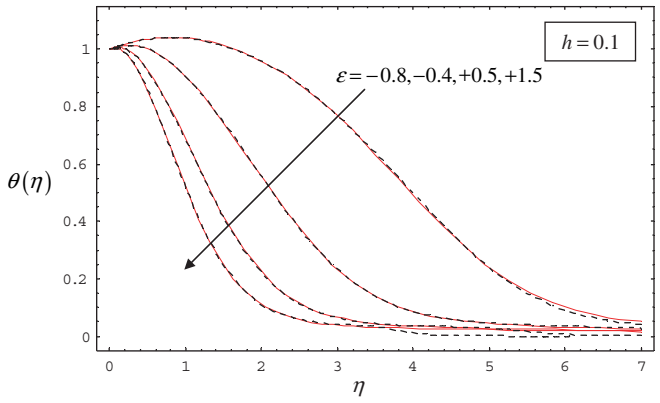

Fig. 9. The numerically "exact" similar temperature profiles (full lines) corresponding to $h = 0.1$ and four different values of ε as compared to those obtained from Eqs. (41) and (48) by truncating the series to polynomials of degree 13.

6. Discussion and conclusions

The goal of the present section is to discuss the results obtained above for $\lambda = -1/3$, in the context of the results reported by other authors for different values of the power-law exponent λ of the wall temperature distribution (1).

The similar downstream velocity $f'(\eta)$ and the similar temperature $\theta(\eta)$ involved in the boundary value problem (2) and (3) can easily be uncoupled from each other with the aid of Eq. (2b). Presumably on this reason the most of the previous investigations have been concerned with the uncoupled form of (2) and (3), i.e. with the "f-problem" specified by equations

$$f''' + (1+\lambda) f \cdot f'' + 2\lambda(1 - f')f' = 0, \tag{50}$$

$$f(0) = 0, \quad f'(0) = 1 + \varepsilon, \quad f'(\infty) = 1. \tag{51a, b, c}$$

In this case, for a given value of λ, the existence domain of the solutions has to be specified in the parameter plane (ε, s) where

$$s \equiv f''(0), \tag{52}$$

denotes the similar wall shear stress of the flow. This quantity is related to the similar temperature gradient (6) by the relationship

$$s = \varepsilon h. \tag{53}$$

It is important to underline here that the elimination of θ from Eqs. (2) and (3) is only possible for non-vanishing values, $\varepsilon \neq 0$, of the mixed convection parameter. In the forced convection case, $\varepsilon = 0$, the f-problem (50) and (51) admits a single "true" solution only. It is given by Eq. (10) and corresponds to $s = 0$ (see also point 2 below).

The reason that our present approach was focused mainly on the similar temperature $\theta(\eta)$ instead of the velocity $f'(\eta)$ is twofold, namely (i) the existence of the additional thermodynamic constraint (4) for the physically acceptable solutions for $\theta(\eta)$ and (ii) the value $\varepsilon = 0$ of the mixed convection parameter is a singular point of the transformations (2b) and (53) connecting θ to f' and h to s, respectively.

In order to be able to discuss the solutions of the f-problem (50) and (51) for $\lambda = -1/3$, the existence domain of the solutions of problem (2)–(4) as shown in Fig. 4 has first to be mapped onto the parameter plane (ε, s) by taking into account Eq. (53) and the feature (ii) mentioned above. The result of this mapping is shown in Fig. 10 and can be summarized as follows:

1. The solution domain of the f-problem (50) and (51) extends from the border curve $s = s_{\min}(\varepsilon)$ to the region of the parameter plane (ε, s) above it. The point $(\varepsilon, s) = (-1, 0)$ does not belong to the solution domain.
2. Except for the origin $(\varepsilon, s) = (0, 0)$, the solutions corresponding to the points of the s-axis in the range $s \geqslant -0.6945$, i.e. the domains AC and BD, are not

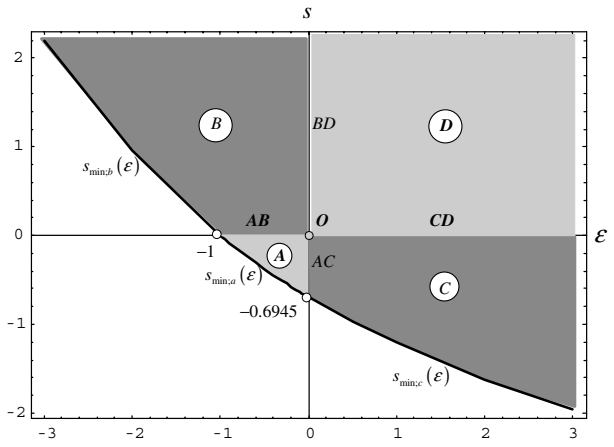

Fig. 10. For $\lambda = -1/3$ the solution domain of the boundary value problem (50) and (51) extends from the border curve $s = s_{\min}(\varepsilon)$ to the region of the parameter plane (ε, s) above it. The point $(\varepsilon, s) = (-1, 0)$ does not belong to the solution domain and the solutions corresponding to the points of $AC \cup BD$ are artifacts. The subdomain of physical solutions $A \cup AB \cup O \cup CD \cup D$ is highlighted by grey. The subdomain of non-physical solutions $B \cup C$ is highlighted by dark grey.

"true" solutions of the f-problem, but artifacts originating from the fact that the elimination of θ from Eqs. (2) and (3), which led to Eq. (50), is only allowed for $\varepsilon \neq 0$.

3. The physical solutions of the f-problem which lead via Eq. (2) to non-negative temperature profiles $\theta(\eta)$ correspond to the points of the subset

$$A \cup AB \cup O \cup CD \cup D, \tag{54}$$

4. The solutions of the f-problem (50), (51) which correspond to the points of the subset

$$B \cup C \tag{55}$$

lead via Eqs. (2) to temperatures $\theta(\eta)$ which become negative in some ranges of the similarity variable η and thus they are non-physical.

As an illustration, in Figs. 11a and 11b some non-physical solutions of the f-problem and the corresponding temperature profiles (which do not satisfy the positiveness condition 8b) are shown.

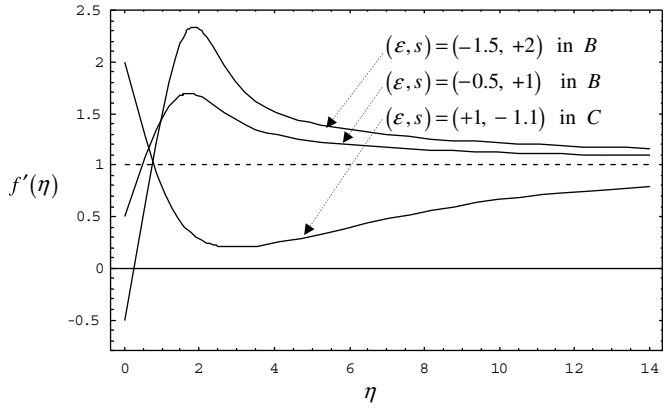

Fig. 11a. Shape of the velocity profiles $f' = f'(\eta)$ for different points (ε, s) belonging to the non-physical subdomains B and C of the parameter plane shown in Fig. 10.

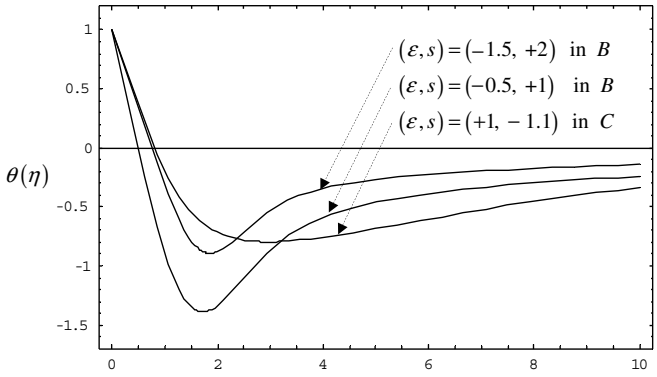

Fig. 11b. Shape of the non-physical temperature profiles $\theta = \theta(\eta)$ associated with the velocity profiles shown in Fig. 11a.

The above results obtained for the solutions of the f-problem (50), (51) for $\lambda = -1/3$ can now be compared easily with those reported by other authors for different values of the power-law exponent λ.

As reported recently by Guedda [14] the f-problem (50), (51) admits for $-1 < \lambda < 0$ an infinite number of solutions for any specified value of $-1 < \varepsilon < 1/2$. This is in full agreement with the present results. In addition, in the case $\lambda = -1/3$ the solution domain extends to the whole ε-axis, except for the point $(\varepsilon, s) = (-1, 0)$ as shown in Fig. 10. This domain is, bounded from below by the border curve $s_{\min}(\varepsilon)$. Moreover, the solutions are only physical in the subdomain (54) and non-physical in (55) as explained above. It is also worth mentioning here that for $\varepsilon < -1$, the velocity profiles $f'(\eta)$ of the subdomain B include backflow regions where $f'(\eta)$ is negative (see Fig. 11a). This, obviously, is not surprising since the negative values of ε correspond to adverse mixed convection flows and when in this range $|\varepsilon|$ is large enough, a flow reversal can arise. On the other hand these solutions are non-physical (in the case $\lambda = -1/3$) since they violate the thermodynamic requirement (4) of the positiveness of θ.

Brighi and Hoernel [15] have proved that the f-problem (50), (51) admits for $\lambda > 0$ unique convex solutions for $-1 < \varepsilon < 0$ and unique concave solutions for $\varepsilon > 0$. Surprisingly, a part of these results hold also in the case $\lambda = -1/3$. Although our solutions are not unique (see Fig. 10), those associated with the vanishing value $s = 0$ of the wall shear stress (subdomains AB and CD of Fig. 10) are convex for $-1 < \varepsilon < 0$ and concave for $\varepsilon > 0$, respectively. The numerical evidence for this feature is given by Fig. 1.

In the past the considerable research effort has been directed on the particular case $\lambda = 0$ of the f-problems (50) and (51). In the present context of the porous media, $\lambda = 0$ corresponds to an isothermal surface. This case has first been investigated by Merkin [2,3]. On the other hand the problem (50) and (51) with $\lambda = 0$ and $\varepsilon < -1$ also occurs in connection with the boundary-layer flow induced in a uniform stream by a plane wall which moves in the

upstream direction with a constant velocity. In this context, the case $\lambda = 0$ of the f-problem has first been investigated by Hussaini and Lakin [18] and Hussaini et al. [19]. The main result of these investigations is that the ε-range of the existence domain of the solutions is bounded from below, $-1.354 = \varepsilon_b(0) < \varepsilon < 0$ and that within this range dual solutions exist for $-1.354 = \varepsilon_b(0) < \varepsilon < -1$, while for $-1 < \varepsilon < 0$ the f-problem admits unique solutions. Recent investigations by Aly et al. [12] have shown that the dual character of the solution found for ($\lambda = 0$ and $-1.354 = \varepsilon_b(0) < \varepsilon < -1$) still persists also for ($\lambda = -0.1$ and $-1.3241 = \varepsilon_b(-0.1) < \varepsilon < 0.5$), as well as for ($\lambda = +0.05$ and $-1.364 = \varepsilon_b(+0.05) < \varepsilon < \infty$). As our present results show, the lower bound ε_b is shifted for $\lambda = -1/3$ to $-\infty$ and the multiplicity of the non-unique solutions increases from 2 to (a non-denumerable) infinity. At the moment it is not exactly known where in the range $-1/3 < \lambda \leqslant 0$ the crossover from the dual solutions to the family of infinite solutions takes place. Our present considerations also emphasizes that all the investigations of the mixed convection problem (2) and (3) which are carried out on its uncoupled form (50) and (51) have to be supplemented by the condition of the non-negative temperatures,

$$\theta(\eta) = \frac{f'(\eta) - 1}{\varepsilon} > 0 \quad \text{for } 0 \leqslant \eta < \infty \quad \text{and} \quad \varepsilon \neq 0, \tag{56}$$

as a physical requirement of the principles of thermodynamics.

Acknowledgement

We are indebted to Professor D.B. Ingham for encouraging our present research work.

Appendix A

The dimensional velocity and temperature fields $\mathbf{v} = (u, v, 0)$ and $T(x, y)$ of the mixed convection problem considered by Aly et al. [12] are obtained from the solution $f = f(\eta)$ and $\theta = \theta(\eta)$ of the boundary value problem (2) and (3) as follows:

$$u(x,y) = U_0 \cdot \left(\frac{x}{L}\right)^{\lambda} \cdot f'(\eta), \tag{A-1a, b}$$

$$v(x,y) = -\frac{\alpha_m}{L}\sqrt{\frac{Pe}{2}} \cdot \left(\frac{x}{L}\right)^{\frac{\lambda-1}{2}} [(\lambda+1)f(\eta) + (\lambda-1)\eta f'(\eta)]$$

$$T(x,y) = T_\infty + T_0 \cdot \left(\frac{x}{L}\right)^{\lambda} \theta(\eta), \tag{A-2}$$

$$\eta = \sqrt{\frac{Pe}{2}}\left(\frac{x}{L}\right)^{\frac{\lambda-1}{2}} \cdot \frac{y}{L}. \tag{A-3}$$

Here U_0 is a reference velocity, α_m is the effective thermal diffusivity of the medium, ε stands for the ratio of the Darcy-Rayleigh number and the Péclet number,

$$\varepsilon = \frac{Ra}{Pe}, \quad Ra = \frac{\rho g \beta K L T_0}{\mu \alpha_m}, \quad Pe = \frac{U_0 L}{\alpha_m} \tag{A-4a, b, c}$$

and the other notations are standard.

The wall shear stress $\tau_w(x) = \mu \partial u/\partial y|_{y=0}$ is obtained as

$$\tau_w(x) = \frac{\mu U_0}{L}\sqrt{\frac{Pe}{2}}\left(\frac{x}{L}\right)^{\frac{3\lambda-1}{2}} f''(0) \tag{A-5}$$

and the wall heat flux $q_w(x) = -k_m \partial T/\partial y|_{y=0}$ as

$$q_w(x) = -\frac{k_m T_0}{L}\sqrt{\frac{Pe}{2}}\left(\frac{x}{L}\right)^{\frac{3\lambda-1}{2}} \theta'(0). \tag{A-6}$$

On obvious reason, the quantities $f'(\eta)$, $\theta(\eta)$, $f''(0)$ and $\theta'(0)$ are named similar down stream velocity, similar temperature, similar wall shear stress and similar wall heat flux, respectively.

Appendix B

The solution of the implicit equation

$$y = a + b \cdot G(y), \tag{B-1}$$

where G is a function of y which is analytic for $y = a$, and a and b are independent of y is given by the Lagrange-expansion (see Whittaker and Watson [20], Chapter 7)

$$y = a + \sum_{n=1}^{\infty} \frac{b^n}{n!}\left[\frac{d^{n-1}}{dz^{n-1}} G^n(y)\right]_{z=a}. \tag{B-2}$$

The Lagrange-expansion of an arbitrary function $\Phi = \Phi(y)$ of this y reads

$$\Phi(y) = \Phi(a) + \sum_{n=1}^{\infty} \frac{b^n}{n!}\left\{\frac{d^{n-1}}{dz^{n-1}}\left[G^n(y) \cdot \frac{d\Phi(z)}{dz}\right]\right\}_{z=a}. \tag{B-3}$$

References

[1] P. Cheng, Combined free and forced convection flow about inclined surfaces in porous media, Int. J. Heat Mass Transfer 20 (1977) 807–814.
[2] J.H. Merkin, Mixed convection boundary layer flow on a vertical surface in a saturated porous medium, J. Eng. Math. 14 (1980) 301–313.
[3] J.H. Merkin, On dual solutions occurring in mixed convection in a porous medium, J. Eng. Math. 20 (1985) 171–179.
[4] D.A. Nield, A. Bejan, Convection in Porous Media, second ed., Springer, New York, 1999.
[5] K. Vafai (Ed.), Handbook of Porous Media, vol. I, Marcel Dekker, New York, 2000.
[6] I. Pop, D.B. Ingham, Convective Heat Transfer: Mathematical and Computational Modelling of Viscous Fluids and Porous Media, Pergamon, Oxford, 2001.
[7] A. Bejan, A.D. Kraus, Heat Transfer Handbook, Wiley, New York, 2003.
[8] D.B. Ingham, A. Bejan, E. Mamut, I. Pop (Eds.), Emerging Technologies and Techniques in Porous Media, Kluwer, Dordrecht, 2004.
[9] A. Bejan, I. Dincer, S. Lorente, A.F. Miguel, A.H. Reis, Porous and Complex Flow Structures in Modern Technologies, Springer, New York, 2004.
[10] K. Vafai (Ed.), Handbook of Porous Media, vol. II, Marcel Dekker, New York, 2005.
[11] E.H. Aly, Some Computational Problems in Porous Media, M.Sc. Thesis, University of Leeds, Leeds, 2002.

[12] E.H. Aly, L. Elliott, D.B. Ingham, Mixed convection boundary-layer flow over a vertical surface embedded in a porous medium, Eur. J. Mech.-Fluids 22 (2003) 529–543.
[13] R. Nazar, N. Amin, I. Pop, Unsteady mixed convection boundary layer flow near the stagnation point on a vertical surface in a porous medium, Int. J. Heat Mass Transfer 47 (2004) 2681–2688.
[14] M. Guedda, Multiple solutions of mixed convection boundary-layer approximations in a porous medium, Appl. Math. Lett. 19 (2006) 63–68.
[15] B. Brighi, J.-D. Hoernel, On the concave and convex solutions of mixed convection boundary layer approximation in a porous medium, Appl. Math. Lett. 19 (2006) 69–74.
[16] M. Abramowitz, I.A. Stegun, Handbook of Mathematical Functions, fourth ed., Dover, New York, 1972.
[17] K. Knopp, Theory and Application of Infinite Series, Dover, New York, 1990.
[18] M.Y. Hussaini, W.D. Lakin, Existence and nonuniqueness of similarity solutions of a boundary-layer problem, Q. J. Mech. Appl. Math. 39 (1986) 15–24.
[19] M.Y. Hussaini, W.D. Lakin, A. Nachman, On similarity solutions of a boundary layer problem with an upstream moving wall, SIAM J. Appl. Math. 47 (1987) 699–709.
[20] E.T. Whittaker, G.N. Watson, A Course of Modern Analysis, fourth ed., Cambridge, UP, London, 1962.